INVENTORY OF WASTE MATERIALS FROM SILICON INGOT AND WAFER MANUFACTURING FOR A CIRCULAR PV VALUE CHAIN

Yijiang Xu[a], Gaute Stokkan[a], Anne-Karin Søiland[b], Birgit Ryningen[a], Irene Bragstad[a], Martin Bellmann[a]
a SINTEF Industry, b ReSiTec AS
a Richard Birkelands vei 3, 7034 Trondheim, Norway. b Setesdalsveien 110, 4617 Kristiansand, Norway.

ABSTRACT: Photovoltaics (PV) is one of the most important renewable energy. During the production of Si-based PV panels, large resource flows are generated, and many waste materials are generated. The challenge for recycling is connected to the material properties: The composition, purity and morphology will determine how the current waste should be processed in order to realize the potential value. We have therefore performed a waste inventory for three important material flows occurring from monocrystalline silicon ingot and wafer manufacturing in the PV production value chain: Si kerf from sawing of wafers, silica from crucibles used in CZ-Si ingot pulling and graphite from CZ crystal growth furnaces. A series of characterization and analysis methods, have been used to investigate the chemical composition, phases, size and morphology etc. of the three waste materials. Possible contamination sources were discussed. The waste inventory results give an overview of the materials quality and property, and their potential for recycling and re-use in the PV section and other application fields.
Keywords: Si kerf, Recycling, Materials characterization

1 INTRODUCTION

The PV module market in 2021 [1] showed a significant growth to 183 GW, where 95% is based on the c-Si technology. Among c-Si module, mono-Si is the dominant in the market while mc-Si products reduced to 13%. The upstream silicon ingot and water manufacturing process is very energy intensive, and consume large quantity of raw material and parts, and generate large waste. In the silicon wafer slicing processes, diamond wire sawing, nearly 40% of the high purity silicon become kerf loss waste. The amount of Si kerf waste is estimated to be at around 160, 000 metric ton in 2021. Besides, in the silicon ingot production process, ancillary materials, such as graphite used as crystal growth furnace parts, and silica from fused quartz crucibles turn to waste. According to the recent report [2], the global isostatic graphite consumed in PV filed is estimated around 50, 000 metric tons in 2021. And the silica waste volume reached 205,400 mt in 2019.

The diamond wire sawing (DWS) process has replaced the traditional slurry process for silicon wafer manufacturing. The steel wire are covered with diamond grits by electroplated nickel coating. Silicon bricks which are mounted to a beam are fed into the moving wire web while being bathed in water-based cutting fluid. Depending on the wire thickness, around 35% of silicon is lost as Si-kerf which is dispersed in the water-based cutting fluid. The cutting fluid and the Si-kerf are later separated through a filter press providing a liquid and a solid fraction (Si-kerf filter cake). The investigation and research on recycling these Si kerf for different application has started since 2013 [3], but it is still at its infant stage. It is short of a systematic characterization and inventory of these materials, to clarify the composition, phases, impurities, morphology etc.

In silicon ingot growth furnace, such as Czochralski single crystal furnace, there are about 30 kinds of high purity isostatic graphite parts [4], including vortex, heater, heat shields and insulation components, susceptors, bases for rotation. Graphite used in the hottest sections of the furnace has a lifetime of only about a few months, either due to the structure and property degradation or due to the impurity deposition and formation. This material is currently down-cycled as low-value carbon for example as a reducing agent in smelting operations. In order to recycle it as a high-value material, such as reuse in existing graphite production plants and use for anode materials in lithium-ion batteries, a detailed analysis of these graphite is demanded.

In addition, in Czochralski process for silicon ingot growth, high purity fused quartz crucible is another key component [5]. It is used to hold the silicon melt during ingot production. The crucible has two layers, a bubble containing layer with certain mechanical strength and a bubble-free inner layer. During the CZ-process, the silica goes through a phase change, forming cristobalite on the surfaces. At the same time, bubbles could form and grow in the bubble-free layer after several runs, which is detrimental for the growing ingot. Therefore, the life time of these crucibles is very limited. After cooled down, the remaining silicon is sticked to the bottom part of the crucible, and the crucibles cannot be reused. This waste materials is being landfilled. Some research has been reported [6] to study the silica crucible waste from the multicrystalline silicon ingot growth, and the method for recycling. However, those crucibles are different from the high purity fused quartz crucibles for CZ mono-crystalline silicon regarding the original state, purity and the using condition etc.. Until now, there is no investigation on the used crucibles from CZ Si growth process, regarding the phases, impurity and its potential for recycling etc.

In this work, the materials' quality of three important waste material from silicon-ingot and wafer manufacturing in the PV production value chain: Si kerf from sawing of wafers, silica from crucibles used in crystal pulling and graphite from crystal growth furnaces, has been investigated. The quality is mainly consisted of chemical composition and impurity content, phases, size and morphology of particles in powder form etc.

2 EXPERIMENTAL

2.1 Materials

The materials investigated are summarized in Table I. Si kerf samples with different source and condition are labled with different ID number. While graphite and silica crucible scrap are only from Norway.

Table I: Type, origin, ID and condition of waste materials investigated in this study.

Waste type	Origin	ID	Condition
Si-kerf dry (1x)	Norway	RST-ODIN-0921	Dried
Si-kerf dry (3x)	Asia	RST-HAN-0120/-MING-020/-SONG1-0721	Dried
Hot-zone graphite	Norway	RST-ODIN-C	crushed
Silica crucible scrap	Norway	RST-ODIN-Q-0921	crushed

For the crushed graphite samples, they have been sorted according to their visual appearance: 1: "clean" samples, 2: yellow surface, 3: silver-grey surface, 4: silver with droplet. Here in this work, sample type 1&type 4 will be studied.

For the silica crucible samples, they were categorized as well by 4 different types, as shown in Fig. 1. 1: Clean samples with a white layer on the crucible inner and outer surface, 2: Inner surface with orange and brown dots, while outer surface is white, 3: Outer surface with orange dots and areal spreading, while inner surface is white, 4: Non-flat inner surface with silver-like particles.

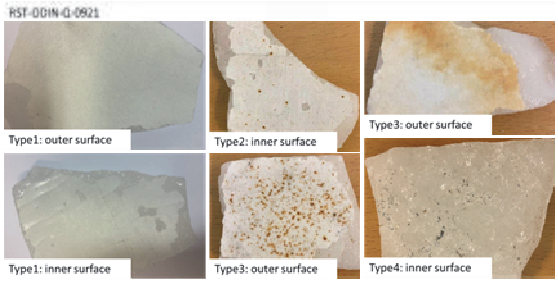

Figure 1: Silica samples and categorization in different types: type 1: white inner and outer surface, type 2: small yellow and black dots at the inner surface, type 3: yellow dots and spread on the outer surface, type 4: silver-like particles on the non-flat inner surface.

2.2 Analysis and Characterization methods

A series of chemical analysis and materials characterization, such as Inductively coupled plasma mass spectrometry (ICP-MS), LECO, X-ray photoelectron spectroscopy (XPS), X-ray diffraction analysis (XRD), light microscopy and scanning electron microscopy, and laser diffraction has been performed.

3 RESULTS

3.1 Silicon kerf

Fig. 2 shows the concentration (in ppmw) of common dopant elements (B, Ga and P) in different Si-kerf samples measured by ICP-MS. The B content in ODIN source samples and most other source samples is around 0.35 to 0.4 ppm. Ming-0120 has slightly higher B, which reaches 0.6 ppm. The Ga content is in the range of 0.05 to 0.65 ppm depending on the source. Generally, ODIN source has higher Ga concentration. For P, the highest content is 15 ppm while lowest is 4 ppm, which is much higher than B and Ga. Comparing the dry samples from different sources, it can be seen that for Asian sources the P content is higher than for the ODIN sources.

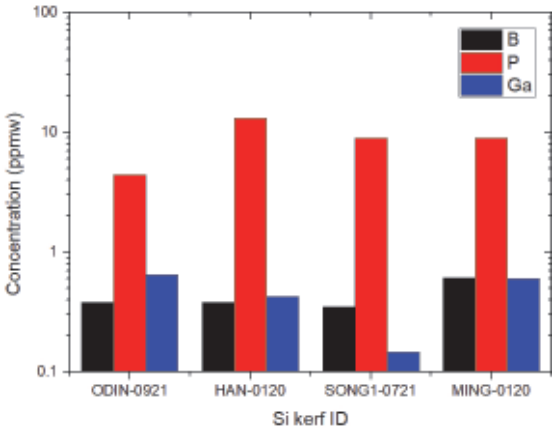

Figure 2: Content of common dopants (B, Ga and P) in different Si-kerf samples measured by ICP-MS.

The metal contaminations, such as Al, Fe, and Ni, determined by ICP-MS are shown in Fig. 3. ODIN source sample has the highest Al (~0.72 wt.%), while the three Asian samples have much lower Al (<1000 ppm), especially SONG1 only has 10 ppm. Al contamination in ODIN source should be mainly from aluminium tri-hydroxide used as beam material in the DWS process. Ming has a very high Fe concentration (~1000 ppm), while other samples have less than 100 ppm Fe. The Fe content in ODIN source samples is lower than that in Asian samples. Fe contamination could come from the steel wire or other steel-made equipment/tools in the filtration and drying process. In addition, Ni is a common contamination element, due to the use of electroplated nickel coating on the steel wire. Typical Ni content is 100-200 ppm.

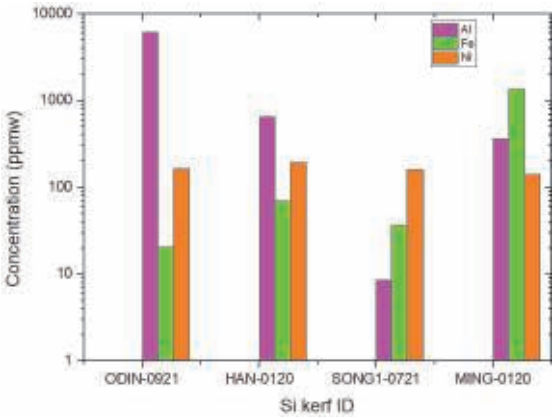

Figure 3: Content of metal impurities (Al, Fe, Ni) in different Si-kerf samples measured by ICP-MS.

Table II shows the carbon and oxygen content measured by LECO. The typical carbon content for most of the samples is around 1-2 wt.%, while SONG1 is more than double this. Carbon may come from the organic compound in the cutting fluid. The oxygen content is about 4-5 wt.%.

Table II Carbon and oxygen content in different Si kerf samples measured by LECO.

Sample-ID (wt.%)	RST-ODIN-0921	RST-HAN-0120	RST-MING-0120	RST-SONG1-0721
Carbon	2.0	2.0	1.0	4.4
Oxygen	4.2	4.3	4.8	5.6

Fig. 4 shows an SEM image of RST-ODIN-0921-dry Si-kerf sample. It is seen that the Si-kerf consists of ribbon-like, irregular shaped angular particles, agglomerates, and nano-sized particles. The ribbon shaped particles are up to around 4 µm long.

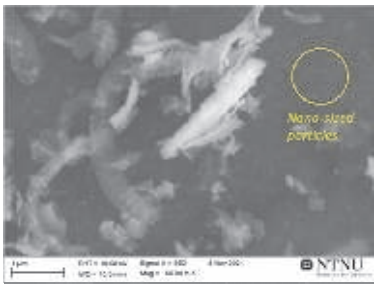

Figure 4: SEM images of RST-ODIN-0921-dry Si-kerf sample.

The particle size distribution (spherical equivalent) of two representative Si kerf samples from Norway and Asia measured by laser diffraction analysis is shown in Fig. 5. As can be seen, ODIN-0921 has more small particles with size below 0.34 µm, and more particles in the range of 0.66-1.8 µm, but less big particles larger than 2 µm.

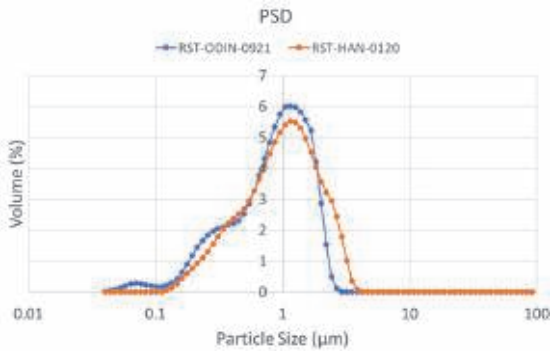

Figure 5: Particle size distribution of 2 Si-kerf samples (RST-ODIN-0921 and RST-HAN-0120) measured by laser diffraction method.

3.2 Graphite

The ash content of graphite sample is 0.16% and 4.1% respectively for sample 1 and sampel4. The metal impurity content in the graphite was calculated from the impurity content measured in the ash by ICP-MS, and the results are listed in Table III. It can be seen that the highest impurity is Si, which is at 0.39 wt.% and 10.9 wt.% in graphite sample 1 and sample 4. Other impurities are in ppm level. Ca and Co are slightly higher in sample 4.

Table III: Impurity content in the graphite measured by ICP-MS of ash samples.

	Si wt%	Ca_p pmw	Al_p pmw	Fe_p pmw	Co_p pmw	Ni_p pmw	Ti	B_p pmw	P_{pp} mw
#1	0.39	4.7	1.3	2.0	5.5	0.2	0.2	0.1	6.7
#4	10.9	21.8	0.6	2.1	41.1	0.7	0.3	0.2	10.2

Fig. 6 shows the XRD results of graphite sample 4. Both Si and SiC are identified on the surface. The surface is further characterized by SEM. Two representative Secondary electron images are shown in Fig. 7. In Fig. 7a, we see a region with flat surface and a region with rough surface. The flat region is consisted of Si grains. While in the rough region, there are several phases with different morphologies. From magnified images of Fig. 7b, it shows that some facetted particles are imbedded inside some matrix, while only exposing some surfaces, which is SiC. At the same time, there are some small spherical shaped phases and irregular particles on the surface.

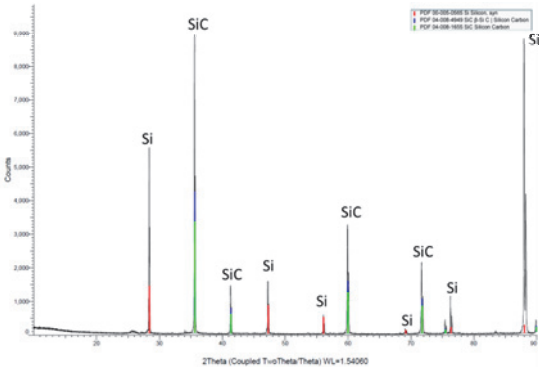

Figure 6: XRD results of the surface of graphite type 4.

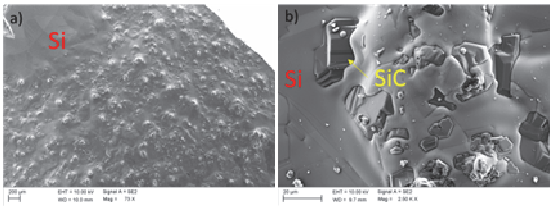

Figure 7: SEM secondary electron image of graphite type 4 sample surface.

3.3 Silica

Fig. 8 shows the XRD results of powder sample of silica type 4, which is similar to the pattern obtained for the other three types. A sharp cristobalite peak is observed, which is the only crystalline phase been detected. Si phase was not detected by current XRD, probably due to the small volume fraction. There is a bump at $2\theta=23^{o}$, which corresponds to the amorphous silica phase.

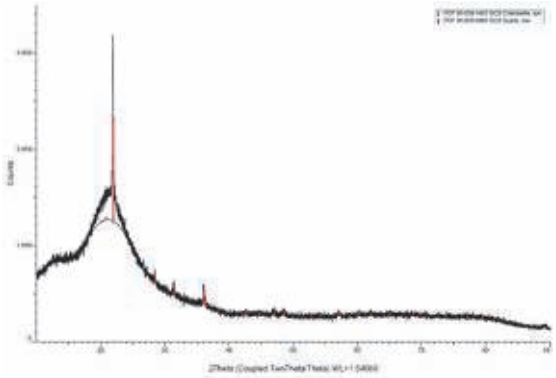

Figure 8: XRD results of milled powder sample of silica sample type 4. Same pattern was obtained for the other 3 sample types as well.

The impurity content determined by ICP-MS is shown in Table IV. The highest impurity is Ca, which is much higher than the typical amount in the new crucibles for CZ process. Co is around 21.4 ppm, which is also higher than the typical value (<0.01 ppm), which could be a result from contamination during the milling process. Similar for Fe, the samples could have been contaminated during crushing process if steel tools have been used. Comparing the 4 samples, it can be seen that type 3 has much higher Al content than the other 3, which are almost the same as in the original quartz sand and new crucible.

Table IV Impurity content (ICP-MS) in the 4 categorized silica samples. All values in ppmw.

#	Na	Al	P	Ca	Ti	Fe	Co	Ba	B
1	11.8	16.7	1.4	518.4	6.7	10.1	25.2	2.1	0.2
2	13.4	10.6	0.6	433.7	6.2	2.4	24.0	1.4	0.6
3	30.1	135.4	1.5	403.5	2.7	37.0	17.4	1.1	<0.2
4	25.0	7.5	1.1	431.2	2.0	26.6	19.0	1.1	<0.2

4 DISCUSSION

For recycling of Si kerf back into the PV value chain as new feedstock, the contamination level is an important parameter. A further refining process is needed to reduce the impurity level to the required amount. Besides, the original wafer sawing process could be optimized to reduce and avoid the contamination of some impurity such as Al and Fe.

Use of Si-kerf in other application or products can be another way to recycle. For example, as feedstock for metallurgical Si production, alloying into Al-Si alloys, and Li-ion battery. The processability will also depend on morphology and surface conditions. It is seen that some differences exist between materials in terms of particle size and surface area.

The graphite is commonly contaminated with Si, SiC etc. The ash content with relatively clean surface graphite is acceptable, while the one with contaminated surface is relatively high. The generally low levels of Ni and Co are promising for typical graphite uses, such as isostatic graphite products and Li-ion battery application.

The differences in impurity concentration between the types are not significant, except type 3 which has an order of magnitude higher Al concentration. The original of high Al in type 3 needs to be further investigated. Ca is also very high in all samples. The recycling and reuse of those waste materials are less explored.

5 CONCLUSIONS

A detailed characterization and analysis of 3 waste materials from solar cell CZ-Si ingot and wafter production process have been performed, including Si kerf, graphite and silica crucibles.

Si-kerf is consisted of ribbon like, irregular shaped angular particles, agglomerates, and nano-sized particles. In Si kerf, the Si concentration is about 92 wt.%, while the main impurities are C (~1-2 wt.%), O (~4-5 wt.%), metallic elements (Al, Ca, Ni, Fe etc.) and doping elements (P, B, Ga).

Graphite contains mainly Si and surface infiltrations of SiC originating from the chemical reactions inside the furnace. The ash content for type 1 graphite is 0.16 %, which is quite low. Other detected impurities are at much lower levels, Ca and Co could reach 20-40 ppm in type 4 and are ~5ppm in type 1. P is about 10 ppm. Other element like Al, Fe Ni, Ti B are below 1ppm.

Silica is mainly present in the form of amorphous silica and crystalline cristobalite. In type 4, it can contain silicon. Ca has the highest level (~500 ppmw) among other impurities. Other impurities like Na, Al, P, Ti, Fe, Co, Ba and B are also present but at much lower levels (1-40 ppmw).

6 ACKNOWLEDGMENT

This project has received funding from the European Union's Horizon 2020 research and innovation programme under grant agreement number 958365.

7 REFERENCES

[1] M. Fisher, M. Woodhouse, S. Herritsch, J. Trube, International technology road map for photovoltaic (ITRPV), 2022.
[2] SPECIAL GRAPHITE MARKET - GROWTH, TRENDS, COVID-19 IMPACT, AND FORECASTS (2022 - 2027) Industry Report, mordor intelligence 2021.
[3] K. Tomono, Separation and Purification Technology 120 (2013) 304.
[4] O. Anttila, Handbook of Silicon Based MEMS Materials and Technologies (Third Edition), 2020
[5] A. Hirsh, Journal of Crystal Growth 570 (2021) 126231.
[6] Y. Zhou, Refractories and Industrial Ceramics 54 (2014) 489.